Journal of Controlled Release 172 (2013) 513–522

Contents lists available at ScienceDirect

Journal of Controlled Release

journal homepage: www.elsevier.com/locate/jconrel

Noninvasive imaging oral absorption of insulin delivered by nanoparticles and its stimulated glucose utilization in controlling postprandial hyperglycemia during OGTT in diabetic rats

Er-Yuan Chuang [a,1], Kun-Ju Lin [b,c,1], Fang-Yi Su [a,1], Fwu-Long Mi [d], Barnali Maiti [a], Chiung-Tong Chen [e], Shiaw-Pyng Wey [b], Tzu-Chen Yen [c], Jyuhn-Huarng Juang [f], Hsing-Wen Sung [a,*]

[a] Department of Chemical Engineering/Institute of Biomedical Engineering, National Tsing Hua University, Hsinchu, Taiwan, ROC
[b] Healthy Aging Research Center, Department of Medical Imaging and Radiological Sciences, College of Medicine, Chang Gung University, Taoyuan, Taiwan, ROC
[c] Department of Nuclear Medicine and Molecular Imaging Center, Chang Gung Memorial Hospital, Taoyuan, Taiwan, ROC
[d] Department of Biochemistry, School of Medicine, College of Medicine, Taipei Medical University, Taipei, Taiwan, ROC
[e] Institute of Biotechnology and Pharmaceutical Research, National Health Research Institutes, Zhunan, Miaoli, Taiwan, ROC
[f] Division of Endocrinology and Metabolism, Chang Gung University and Chang Gung Memorial Hospital, Taoyuan, Taiwan, ROC

ARTICLE INFO

Article history:
Received 1 February 2013
Accepted 12 May 2013
Available online 21 May 2013

Keywords:
Diabetes mellitus
Postprandial hyperglycemia
Oral insulin absorption
Glucose utilization
Chitosan-γPGA–EGTA nanoparticles

ABSTRACT

This work examined the feasibility of preparing a pH-responsive nanoparticle (NP) system composed of chitosan and poly(γ-glutamic acid) conjugated with ethylene glycol tetraacetic acid (γPGA–EGTA) for oral insulin delivery in diabetic rats during an oral glucose tolerance test (OGTT). OGTT has been used largely as a model to mimic the period that comprises and follows a meal, which is often associated with postprandial hyperglycemia. Based on Förster resonance energy transfer (FRET), this work also demonstrated the ability of γPGA–EGTA to protect insulin from an intestinal proteolytic attack in living rats, owing to its ability to deprive the environmental calcium. Additionally, EGTA-conjugated NPs were effective in disrupting the epithelial tight junctions, consequently facilitating the paracellular permeation of insulin throughout the entire small intestine. Moreover, results of positron emission tomography and computer tomography demonstrated the effective absorption of the permeated insulin into the systemic circulation as well as promotion of the glucose utilization in the myocardium, and skeletal muscles of the chest wall, forelimbs and hindlimbs, resulting in a significant glucose-lowering effect. Above results indicate that as-prepared EGTA-conjugated NPs are a promising oral insulin delivery system to control postprandial hyperglycemia and thus may potentially prevent the related diabetic complications.

1. Introduction

Blood glucose levels in diabetic patients often increase promptly and significantly after a meal, possibly related to the development of diabetic complications [1]. As the most effective glucose-lowering agent, insulin can stimulate glucose uptake in skeletal muscles, myocardium, and other tissues in order to control glucose homeostasis [2]. Although subcutaneous (SC) administration of insulin remains the most prevalent means of treating diabetic patients, its patient compliance is poor, owing to their phobia of needles and local pain [3–5].

Alternatively, oral delivery of insulin is a promising means of improving compliance among diabetic patients. However, the bioavailability of insulin *via* oral ingestion is limited, owing to its presystematic degradation and the absorption barriers posed by the intestinal epithelium [3]. To address these limitations, our recent work developed a pH-responsive nanoparticle (NP) system comprising chitosan (CS) and poly(γ-glutamic acid) conjugated with ethylene glycol tetraacetic acid (γPGA–EGTA) for oral insulin delivery [6]. According to those results, the CS/γPGA–EGTA NPs (EGTA-conjugated NPs) could inhibit the proteolytic degradation of insulin and improve its paracellular permeability *in vitro*, as well as enhance the oral bioavailability of insulin in fasting diabetic rats.

As is well known, postprandial hyperglycemia is a more sensitive indicator of diabetic control than fasting glucose levels [7]. The oral glucose tolerance test (OGTT) has been used as a model to mimic the postprandial state of hyperglycemia as well as provides information on the glucose-lowering effect as a consequence of insulin action on the glucose utilization [8].

We hypothesize that insulin absorbed into the systemic circulation, as delivered by the EGTA-conjugated NPs orally, can effectively

* Corresponding author at: Department of Chemical Engineering, National Tsing Hua University, Hsinchu 30013, Taiwan, ROC. Tel.: +886 3 574 2504.
E-mail address: hwsung@che.nthu.edu.tw (H.-W. Sung).
[1] The first three authors (E.Y. Chuang, K.J. Lin and F.Y. Su) contributed equally to this work.

0168-3659
http://dx.doi.org/10.1016/j.jconrel.2013.05.006

promote the glucose utilization and then control the postprandial hyperglycemia during OGTT in diabetic rats. The ability of γPGA–EGTA to inhibit insulin from enzymatic degradation was also evaluated *via* an *in vivo* imaging system (IVIS), based on the concept of Förster resonance energy transfer (FRET). Effects of the EGTA-conjugated NPs on disrupting the ultra-structures of epithelial tight junctions (TJs) and enhancing the intestinal absorption of insulin were visualized directly *in vivo* by transmission electron microscopy (TEM) and confocal laser scanning microscopy (CLSM), respectively. Biodistribution of the absorbed insulin and its subsequent stimulation of glucose uptake were imaged noninvasively by using positron emission tomography (PET)/computer tomography (CT). Their pharmacokinetic (PK) and pharmacodynamic (PD) profiles during OGTT were also analyzed.

2. Materials and methods

2.1. Preparation and characterization of EGTA-conjugated NPs

The 85% deacetylated CS (MW 60 kDa) was purchased from Koyo Chemical Co. Ltd. (Japan), whereas γPGA (MW 100 kDa) was acquired from Vedan Co. (Taichung, Taiwan). Insulin and EGTA were obtained from Sigma-Aldrich (St. Louis, MO, USA). The γPGA–EGTA conjugate was synthesized based on the procedure described in our previous study [6]. Insulin-loaded EGTA-conjugated NPs were prepared using an ionic-gelation method. Briefly, bovine insulin (2 mg/mL, 0.5 mL) was premixed with an aqueous CS solution (1.2 mg/mL, 4 mL, pH 6.0) in the presence of sodium tripolyphosphate (TPP, 1 mg/mL, 0.5 mL) by magnetic stirring at 4 °C for 15 min. Subsequently, the mixed solution was added, *via* flush mixing with a pipette tip, into an aqueous γPGA–EGTA solution (4 mg/mL, 0.5 mL, pH 7.4) and then blended thoroughly at room temperature to form the test NPs. Finally, the obtained NPs were collected *via* centrifugation at 8000 rpm for 50 min, resuspended in deionized (DI) water, and freeze-dried with trehalose (*i.e.*, a cryoprotective agent) for further use [9].

The particle size and zeta potential of the as-prepared NPs were measured by dynamic light scattering (Zetasizer 3000HS, Malvern Instruments Ltd., Worcestershire, UK). The loading efficiency and loading content of insulin in NPs were determined by assaying the amounts of free insulin in supernatants by using high-performance liquid chromatography [6]. The drug loading efficiency (LE) and loading content (LC) were calculated as shown below [5].

$$\mathrm{LE}(\%) = \frac{\text{Total amount of insulin added} - \text{free insulin}}{\text{total amount of insulin added}} \times 100\%$$

$$\mathrm{LC}(\%) = \frac{\text{Total amount of insulin added} - \text{free insulin}}{\text{weight of NPs}} \times 100\%$$

2.2. Detection of insulin degradation by FRET analyses

FRET involves the non-radiative transfer of energy from the excited state of a donor to the empty levels of an acceptor placed in close proximity (<10 nm), and, subsequently, the conformational changes of proteins can be probed using its efficiency [10]. To detect the degradation of insulin (or its conformational changes) based on FRET, an insulin derivative conjugating the fluorescent cyanine 3 (Cy3) and cyanine 5 (Cy5) moieties (Cy3–insulin–Cy5) was prepared. Briefly, equimolar N-hydroxy-succinimide-functionalized Cy3 and Cy5 (2.6 mg/mL, 0.1 mL, GE Healthcare, Little Chalfont, UK) were reacted with insulin (10 mg/mL, 1 mL, 27.4 IU/mg) at pH 9.5 in an ice bath for 24 h [11]. The unconjugated Cy3 and Cy5 molecules were removed *via* dialysis in distilled water at 4 °C for 3 days. Following dialysis, the obtained Cy3–insulin–Cy5 was lyophilized for the subsequent *in vitro* and *in vivo* degradation studies.

In the *in vitro* study, the synthesized Cy3–insulin–Cy5 (1 mg) was incubated with trypsin (4 mg) in a Krebs-Ringer buffer (KRB, 1 mL, pH 7.4) containing $CaCl_2$ (0.06 mg) with or without γPGA–EGTA (40 mg) at 37 °C for 2 h [12]. Insulin is highly sensitive to trypsin, which is a Ca^{2+}-dependent enzyme present in the intestinal fluid and mucus layer [13]. Next, the degradation of Cy3–insulin–Cy5 was monitored by FRET analyses, in which the donor (Cy3) was excited at 535 nm and the emission spectra of the donor–acceptor were recorded at all wavelengths simultaneously by using a fluorescence spectrometer (Horiba Jobin Yvon, Edison, NJ, USA).

The *in vivo* animal study was conducted in compliance with the "Guide for the Care and Use of Laboratory Animals", which was prepared by the Institute of Laboratory Animal Resources, National Research Council, and published by the National Academy Press in 1996, and approved by the Institutional Animal Care and Use Committee of National Tsing Hua University (protocol number 10046). The enzymatic degradation of insulin was investigated *in vivo* using an intestinal closed-loop method [14]. Briefly, overnight-fasted rats (Wistar, ~250 g, n = 5) were anesthetized *via* the intramuscular injection of Zoletil® (50 mg/kg, Virbac Laboratories, Carros, France). The abdominal cavity of animals was opened by a midline incision, and the small intestine was exposed. A 5-cm segment of the duodenum was then selected for producing a closed loop. The proximal end of the intestinal loop was first tied up, and the Cy3–insulin–Cy5 (2 mg/mL, 0.5 mL) in the absence or presence of γPGA–EGTA (40 mg) was then introduced *via* a syringe. The distal end was subsequently ligated to form a closed loop.

Fluorescent signals of Cy3–insulin–Cy5 in the intestinal loop were acquired by using an IVIS (Xenogen, Alameda, CA, USA). The test animal was irradiated at a wavelength of 535 nm (the excitation wavelength of Cy3) and imaged with an appropriate emission filter (680 nm) to obtain Cy5 images. The fluorescent intensities from regions of interest were quantified using Living Image 3.1 software.

2.3. Ultra-structural examination of the permeability of epithelial TJs

The epithelial TJ permeability was observed directly by examining the ultra-structural changes induced by the EGTA-conjugated NPs at different segments of the small intestine by using TEM. In the work, the loops created in the duodenum, jejunum and ileum were individually treated with the test NPs (2 mg/mL, 0.5 mL). Three hours later, the rats were sacrificed; the intestinal loops were subsequently dissected and washed three times with isotonic saline. Next, the dissected loops were fixed in 4% paraformaldehyde and washed with s-Collidine buffer. To illustrate the paracellular permeability, the fixed loops were further incubated with 2% lanthanum, an electron-dense tracer, for 2 h [15]. After rinsing in s-Collidine and phosphate buffered saline (PBS), tissue samples were processed for TEM examination, as detailed previously [16].

2.4. Structural reorganization of TJs and intestinal absorption of insulin

The fluorescein isothiocyanate-labeled insulin (FITC-insulin) was synthesized [17] and then loaded in the EGTA-conjugated NPs. Next, as-prepared fluorescent NPs were introduced into the intestinal loops created in rats (n = 6), as described above. At 2 h following treatment, three of the studied rats were sacrificed, and their loop segments were dissected to examine the corresponding structural reorganization of TJs and intestinal absorption of insulin. Additionally, to study the recovery of TJ structures after removal of test NPs, the ligations of the intestinal loops created in the other three rats were removed and then eluted with deionized (DI) water thoroughly. Twenty-four hours later, rats were sacrificed, and their intestinal loops were dissected.

The dissected intestinal loops were washed with PBS and then fixed in paraformaldehyde. Following fixation, tissue samples were

embedded in paraffin and sectioned (5 μm in thickness). Non-specific binding was blocked in 5% normal goat serum (Jackson ImmunoResearch Laboratories, West Grove, PA, USA) in PBS for 60 min at 37 °C. Test samples were subsequently treated with primary antibodies (rabbit anti ZO-1, Zymed Laboratories, San Francisco, CA, USA) at a 1:50 dilution for 60 min at 37 °C. After rinsing 3 times with PBS, tissue samples were incubated with Alexa-Fluor-conjugated secondary antibodies (Jackson ImmunoResearch Laboratories) with a 1:100 dilution. Samples were also counterstained with propidium iodide (PI, Invitrogen, Carlsbad, CA, USA) to visualize the nuclei and observe *via* an inverted CLSM (TCS SL, Leica, Germany).

2.5. Toxicity of test NPs

Toxicity of the EGTA-conjugated NPs was evaluated in ICR mice (25–30 g, National Laboratory Animal Center, Taipei, Taiwan). Animals were randomly divided into two groups. The experimental group orally received a daily dose of empty NPs (100 mg/kg, n = 5 for each gender) for 14 days, while the other group without any treatment was used as a control. Animals were fed with normal chow and water *ad libitum*, followed by careful observation for the onset of any signs of toxicity and monitoring for changes in body weight. The mice were then sacrificed, along with their internal organs harvested and examined. For sectional histology, intestine, liver and kidney specimens were fixed in 10% phosphate buffered formalin, embedded in paraffin, cross sectioned at 5 μm and then stained with hematoxylin and eosin (H&E) [18].

2.6. Biodistribution study during OGTT

Biodistribution of the insulin orally delivered by the EGTA-conjugated NPs and the insulin-mediated glucose utilization were noninvasively investigated in the streptozotocin-induced diabetic rats [19] during OGTT by using PET/CT (n = 3). In the work, the diethylene triamine pentaacetic acid (DTPA) conjugated insulin was first synthesized to immobilize gallium-68 (^{68}Ga), a radioisotope suitable for PET imaging [20]. Test NPs were then prepared using the obtained ^{68}Ga-insulin, as mentioned earlier.

To assess the insulin biodistribution administered to diabetic rats, dynamic PET scans were acquired after oral ingestion of free-form ^{68}Ga-insulin or ^{68}Ga-insulin-loaded NPs (30 IU/kg). Three days later, glucose utilization was assessed by orally administering 1 mCi/kg of ^{18}F-2-fluoro-2-deoxy-D-glucose (^{18}F-FDG) together with glucose (0.5 g/kg) to the same diabetic rats at 2 h after oral ingestion of free-form insulin or the insulin-loaded NPs (30 IU/kg), a model of OGTT. Dynamic PET images were then obtained through a PET scanner (Siemens Medical Solutions, Knoxville, TN, USA). The obtained images were reconstructed using the 2D OSEM method (4 iterations and 16 subsets) with attenuation corrections. After PET scanning, whole-body CT images were acquired using NanoSPECT/CT (Bioscan, Washington, DC, USA) with the intravenous Conray contrast enhancement (Mallinckrodt Inc., Saint Louis, MO, USA) to more clearly illustrate the heart, great vessels, liver and kidneys. Image fusion of 3D image-volume-rendering of ^{68}Ga-insulin PET, ^{18}F-FDG PET, and CT scans was then performed *via* the image workstation and PMOD version 3 (PMOD Technologies Ltd., Zurich, Switzerland).

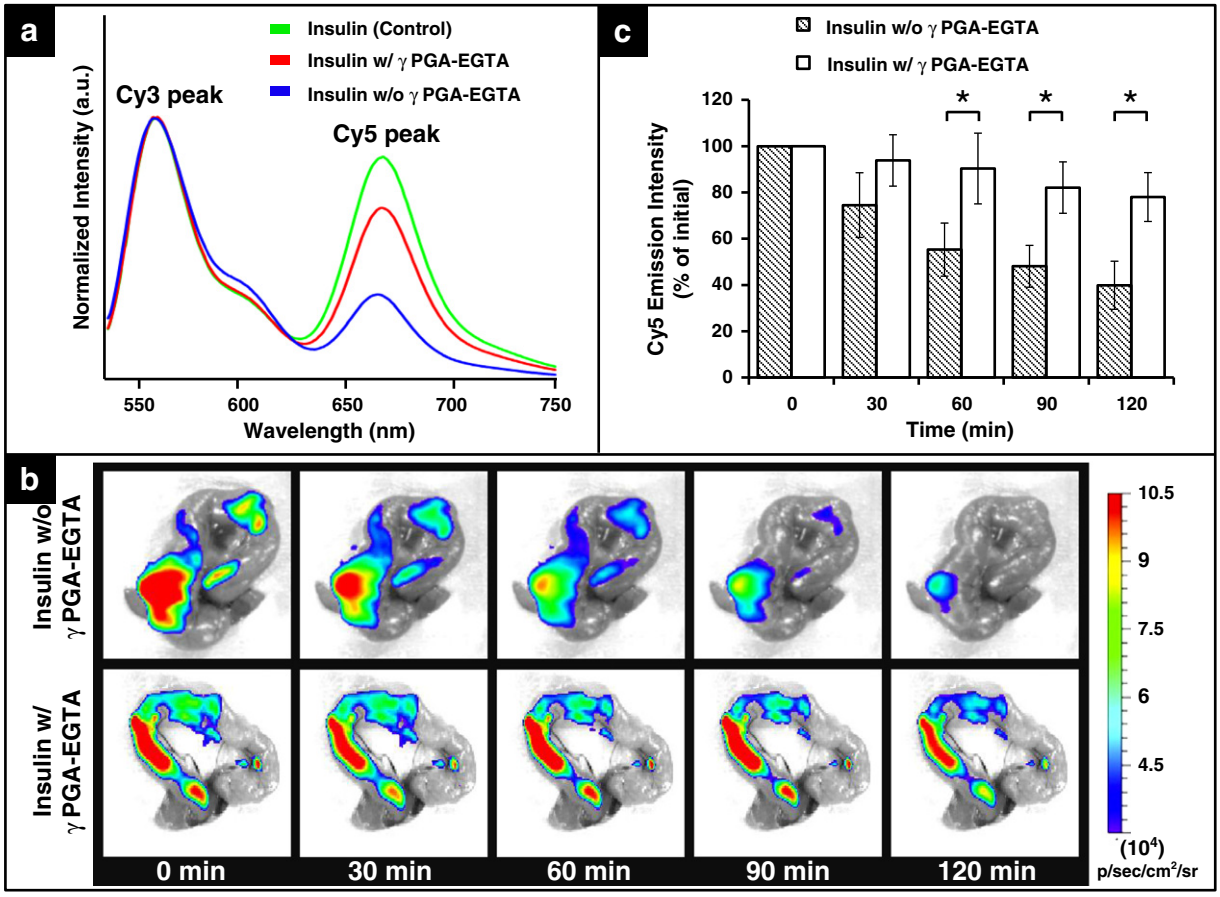

Fig. 1. a) FRET spectra of Cy3–insulin–Cy5 suspensions treated by trypsin with (w/) or without (w/o) γPGA–EGTA, which were normalized to the maximum Cy3 donor peak around 570 nm; (b) Cy5-emission images and (c) the intensities of Cy3–insulin–Cy5 suspensions present in the rat duodenum in the absence or presence of γPGA–EGTA, investigated by an *in vivo* imaging system. *Statistical significance at a level of $P < 0.05$.

2.7. PK/PD study during OGTT

Efficacy and bioavailability of the insulin orally delivered by the EGTA-conjugated NPs during OGTT were examined by randomly dividing diabetic rats into four groups (n = 6 for each studied group). The following formulations were individually administered to the overnight-fasted animals: DI water (oral, empty control), an enteric-coated capsule containing free-form insulin powder (30 IU/kg) and trehalose (oral), an enteric-coated capsule filled with the test NPs containing 30 IU/kg insulin (oral), and a SC injection of free-form insulin solution (5 IU/kg).

To mimic the postprandial state, an oral dose of glucose (1 g/kg) was administered to the animals at 2 h after receiving insulin treatment or DI water. Blood samples were collected from the tail vein, and the blood glucose levels were measured by a glucose meter (LifeScan Inc., Milpitas, CA, USA). Next, plasma insulin levels were analyzed by centrifuging the blood samples (10,000 rpm for 15 min) and then quantifying them by using a bovine insulin ELISA kit (Mercodia AB, Uppsala, Sweden). The relative bioavailability (BA_R) of the absorbed insulin was calculated using the following formula [9]:

$$BA_R = \frac{AUC_{(oral)} \times Dose_{(sc)}}{AUC_{(sc)} \times Dose_{(oral)}} \times 100\%$$

where AUC denotes the total area under the plasma insulin concentration vs. time curve.

2.8. Statistical analysis

The groups were compared using the one-tailed Student's *t*-test (SPSS, Chicago, Ill). All data were presented as a mean value with its standard deviation indicated (mean ± SD). Differences were considered statistically significant when the *P* values were less than 0.05.

3. Results and discussion

OGTT has been used largely as a model to mimic the period that comprises and follows a meal, which is often associated with postprandial hyperglycemia [21]. Insulin can promote the glucose uptake in the insulin-responsive tissues (*e.g.*, skeletal and cardiac muscles), ultimately lowering the postprandial hyperglycemia [22]. This work analyzed the *in vivo* efficacy of the EGTA-conjugated NPs in enhancing the oral absorption of insulin and its subsequent stimulation of glucose utilization by using noninvasive imaging approaches. Such methods can substantially reduce the amount of animals required and limit the inter-subject variability, as the same animals can be imaged at multiple time points [23]. Additionally, image-based analyses of live animal models in a time-resolved manner provide an improved spatial and temporal understanding of dynamic biological processes [24].

3.1. FRET analyses of insulin degradation

Trypsin is a Ca^{2+}-dependent protease present in the small intestine that can degrade insulin [13]. Chelating agents, such as EGTA,

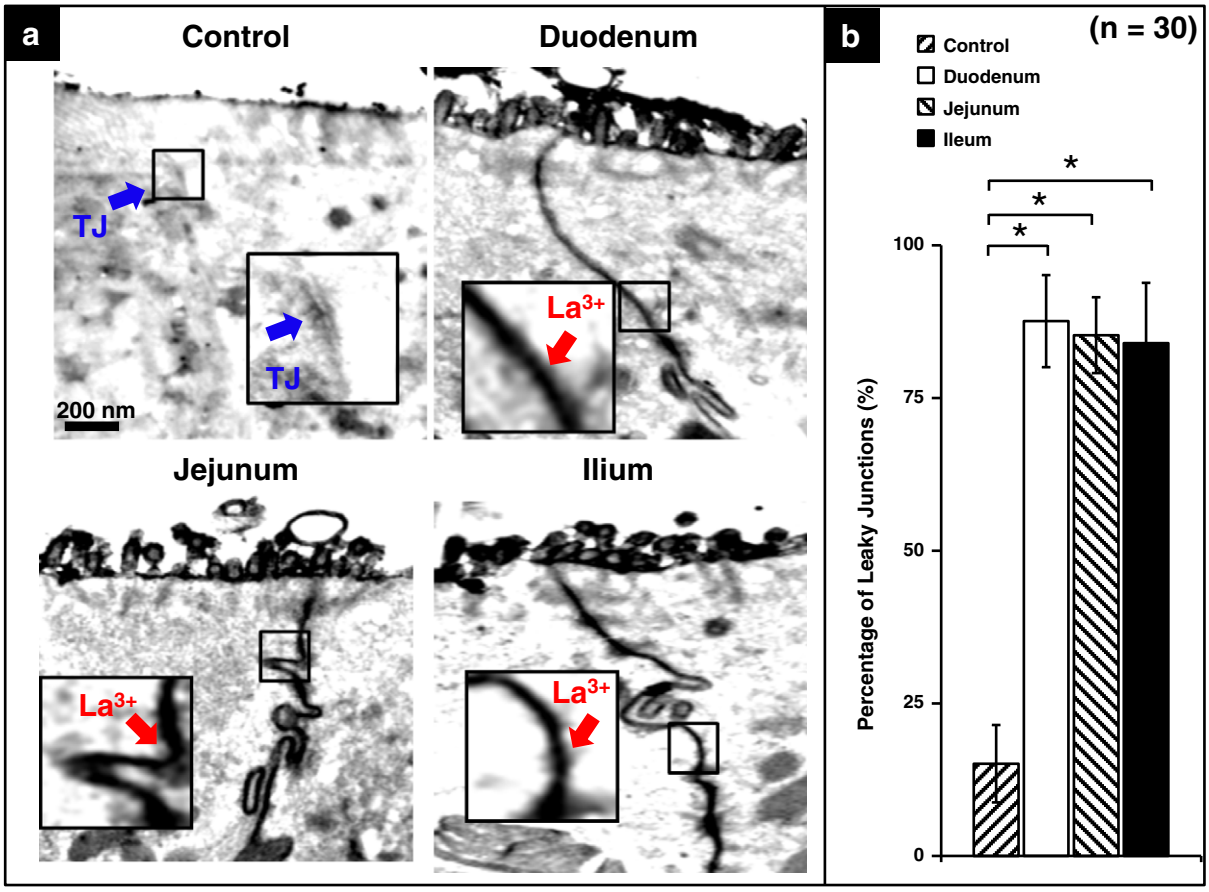

Fig. 2. (a) TEM micrographs of different segments of the rat small intestine before (control) and after treated with test nanoparticles (NPs). The opening of the intact tight junction (TJ, as denoted by the blue arrow) induced by test NPs was revealed by the permeation of lanthanum (La^{3+}, as indicated by the red arrow). Insets show magnified views; (b) percentages of leaky TJs observed at different segments of the small intestine. *Statistical significance at a level of $P < 0.05$.

can deprive the environmental Ca^{2+}, thus limiting the enzymatic activity of trypsin towards insulin [13]. To maintain the concentration of the chelating agent in needed areas, EGTA was conjugated on γPGA; the γPGA–EGTA conjugate was then used to form NPs with CS for oral insulin delivery.

The ability of γPGA–EGTA to protect insulin from the proteolytic attack was studied by synthesizing an insulin-derivative bearing fluorescent Cy3 and Cy5 molecules (Cy3–insulin–Cy5). The Cy3 and Cy5 moieties conjugated on Cy3–insulin–Cy5 constitute a donor–acceptor pair that is appropriate for evaluating the molecular integrity of insulin during degradation, based on their FRET efficiency.

Fig. 1a illustrates the FRET spectra of Cy3–insulin–Cy5 before (control) and after degraded by trypsin *in vitro* with or without γPGA–EGTA, which were normalized to the maximum Cy3 emission peak (~570 nm). According to this figure, the group without γPGA–EGTA (blue curve), had a significantly greater decrease in the fluorescence emission ratio of Cy5/Cy3 than that of the control group (green curve), suggesting a severe proteolytic degradation of Cy3–insulin–Cy5. Conversely, the degradation of Cy3–insulin–Cy5 was markedly reduced in the group with γPGA–EGTA (red curve), owing to its ability to deprive the environmental Ca^{2+}, thus inhibiting the trypsin activity.

The loop created in the duodenum was used in the *in vivo* enzymatic degradation study. As is well known, the pancreas secretes various digestive enzymes, including trypsin, into the duodenum [25]. In the absence of γPGA–EGTA, the fluorescence intensity of Cy3–insulin–Cy5 detected in the intestinal loop decreased significantly with time ($P < 0.05$, Fig. 1b and c), indicating the enzymatic cleavage of Cy3–insulin–Cy5. In contrast, with γPGA–EGTA, changes in fluorescence intensity in the loop over time were limited, thus confirming the protective effect of γPGA–EGTA against the intestinal proteases.

3.2. Characteristics of the EGTA-conjugated NPs

The as-prepared NPs had a mean particle size of 323.1 ± 76.9 nm with a zeta potential of 38.7 ± 4.2 mV. Their insulin loading efficiency and content were 77.4 ± 3.9% and 17.8 ± 2.4%, respectively (n = 6 batches). The test NPs were stable in a pH range of 2.0–7.0. Beyond this range, the particles became unstable and disintegrated, suggesting their pH-responsiveness [26]. Similar characteristics were found for the test NPs containing FITC-insulin or ^{68}Ga-insulin.

3.3. Ultra-structural examination of the permeability of epithelial TJs

In the intestinal pH environments (pH 6.4–7.4), the acidic groups on EGTA are deprotonated [27], thus accelerating their association kinetics of Ca^{2+}. Owing to its chelating effects on Ca^{2+}-dependent adhesion molecules, EGTA can provoke the disruptions of epithelial TJs [28]. As the apical-most member of the junctional complexes, TJs create a primary barrier to the diffusion of macromolecules through the paracellular route in the epithelium [29].

Disruptions of the epithelial TJs induced by the EGTA-conjugated NPs, resulting in the paracellular permeability, were examined by TEM using lanthanum as a tracer. Lanthanum, an electron-dense rare-earth element, has been extensively used to study the permeability of junctional barriers [30]. Intact epithelial TJs prevent lanthanum from permeating into paracellular routes, whereas disrupted or leaky epithelial TJs exhibit lanthanum staining in intercellular spaces [31].

Fig. 2a reveals that before NP treatment (control), the intact epithelial TJs appeared as highly electron-dense structures (as indicated by the blue arrow). After exposure to the EGTA-conjugated NPs, lanthanum infiltrated the paracellular spaces (as denoted by the red

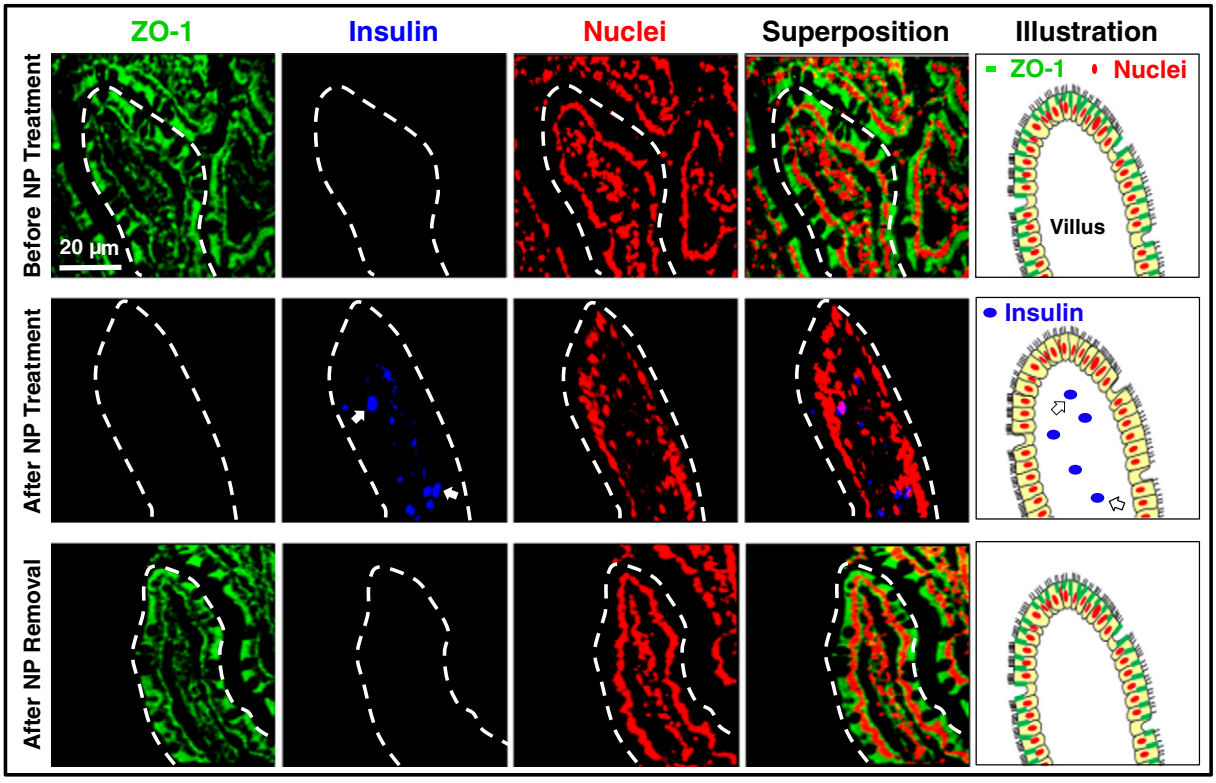

Fig. 3. Fluorescence images taken by a confocal microscope and their corresponding schematic illustrations of rat intestinal villi, showing the change of ZO-1 protein (green color) and the absorption of insulin (blue color) before and after incubation with the insulin-loaded NPs; the images after removal of test NPs are also shown.

arrow), indicating the opening of intercellular junctions, throughout the entire small intestine. The percentages of lanthanum-containing intercellular spaces (or TJ opening) observed in the duodenum, jejunum and ileum segments were 87.6%, 85.3% and 84.0% (n = 30), respectively. Above results suggest that the as-prepared EGTA-conjugated NPs effectively disrupted TJs, thus facilitating the paracellular permeation throughout the entire intestine.

3.4. Structural reorganization of TJs and intestinal absorption of insulin

The cytoplasmic protein, zona occludens-1 (ZO-1), profoundly impacts the structural and functional organization of TJs. Disruptions of ZO-1 at TJs have been observed in response to bacterial toxins or absorption enhancers, which correlates with enhanced paracellular permeability [32]. In this work, the retrieved loop segments were immunofluorescently stained for ZO-1 proteins to examine their TJ structural reorganization and its subsequent intestinal insulin absorption before and after NP treatment.

According to Fig. 3, before NP treatment (control), a honeycomb-like distribution of ZO-1 proteins (green color) in association with the cellular surface was seen (see the last column for illustration). At 2 h after receiving the EGTA-conjugated NPs, ZO-1 proteins disappeared, an indication of TJ disruptions. This observation may be owing to the fact that Ca^{2+}-depletion, caused by the EGTA chelating effect, stimulates ZO-1 trafficking to an acidic endosome and, eventually, to the lysosome for degradation [33].

It has been reported that mucoadhesive CS NPs can adhere to and infiltrate the mucus layer in the small intestine [34]. After adhering to and infiltrating the mucus layer, the NP carriers became unstable and disintegrated owing to their pH sensitivity, subsequently releasing their loaded insulin near the underlying epithelial cells [34]. It is known that the pH environment at the epithelial surface is near neutral [35,36]. The released insulin was then absorbed into the lacteal side of the villi (as denoted by the white arrows in Fig. 3) through the disrupted TJs. After removal of the test NPs, the epithelial villi displayed a pattern of ZO-1 that resembled the control group, suggesting the restoration of TJs through the synthesis of ZO-1, *via* the mRNA translation [37].

3.5. In vivo toxicity study

The gastrointestinal (GI) tract is normally exposed to various potentially detrimental substances, including chemical and bacterial toxins [38]. As our EGTA-conjugated NPs are capable of enhancing the paracellular permeability by opening the epithelial TJs (Fig. 2), it is therefore crucial to study whether this incident could lead to toxicity *in vivo*. In this work, animals were treated with a daily dose of empty EGTA-conjugated NPs for 14 days; the animals without treatment were used as a control group.

Both investigated groups had no apparent clinical symptoms such as diarrhea, fever or other systemic symptoms throughout the study. Over 14 days, body weights of the experimental groups (male and female) increased slightly in a manner similar to those of the control

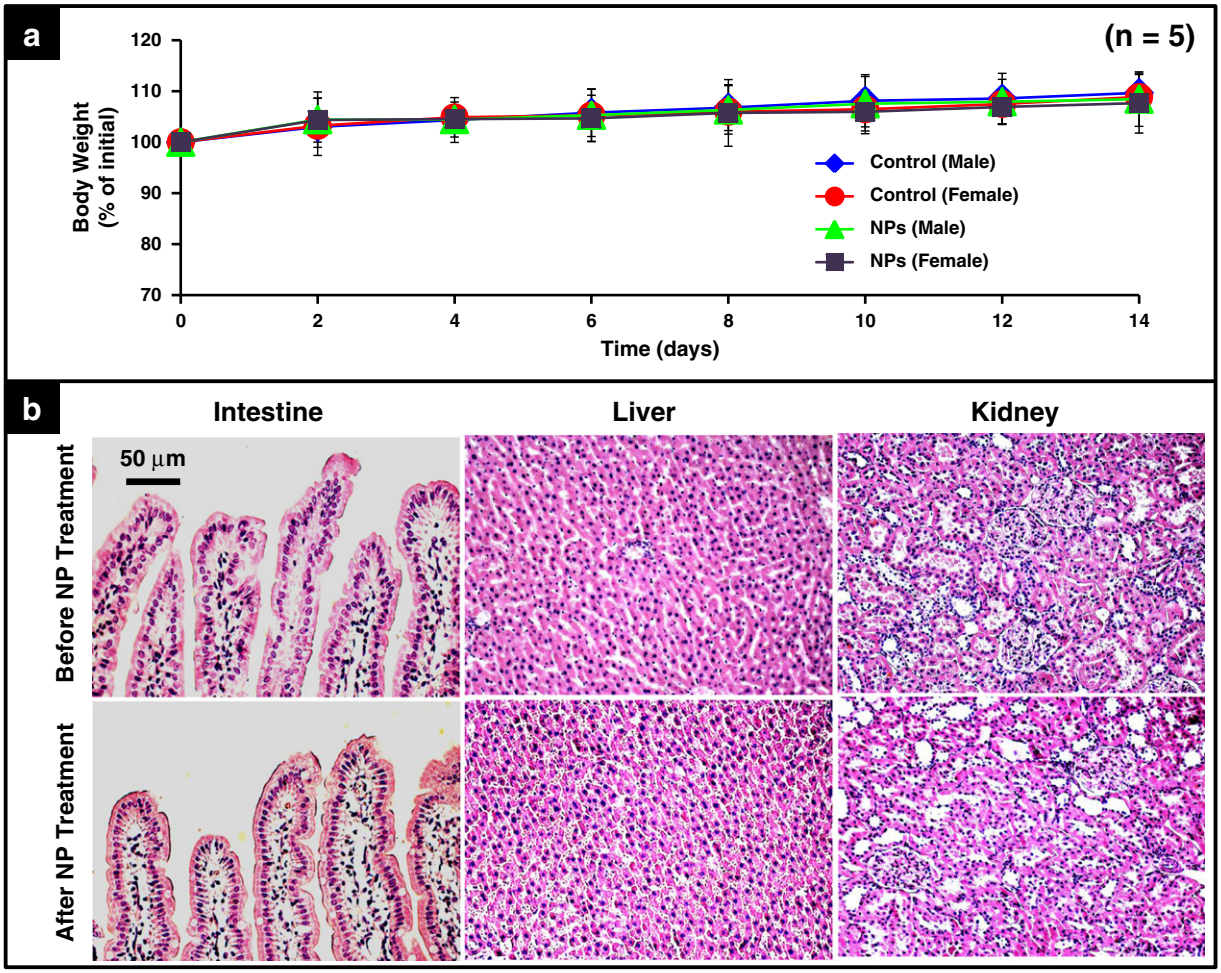

Fig. 4. (a) Changes in body weight with time and (b) representative photomicrographs of the intestine, liver and kidney sections (H&E staining, magnification 200×) of mice before and after treated with test NPs in a dose of 100 mg/kg per day for 14 days.

groups; no gender-related difference was found (Fig. 4a). As is widely recognized, the reduction in body-weight gain is a simple and sensitive index of *in vivo* toxicity [39]. The specific tissue-level toxicological study includes the inflammation (intestine), hepatotoxicity (liver), and nephrotoxicity (kidney) responses [40]. Our histological assessments found no noticeable tissue damages or toxic effects on organs (Fig. 4b).

3.6. Biodistribution during OGTT

PET is a highly effective noninvasive technique for molecular imaging in living animals [41]. Given its high sensitivity and high spatial–temporal resolution, PET is particularly useful in analyzing the time profile of drug accumulation in specific tissues [41,42]. As a well-known PET probe in clinical practice, ^{18}F-FDG is a radiopharmaceutical analog of glucose that can be taken up by metabolically active cells, using facilitated transport similar to that used by glucose [43].

The biodistribution of oral ingestion of free-form ^{68}Ga-insulin was examined by PET; the obtained images were superimposed on the CT scans of test animals for better anatomy localization (Fig. 5). At 2 h following treatment, the coronal section of PET images from retroperitoneum to abdomen revealed that the radioactivity of ^{68}Ga-insulin was present only along the GI tract. Despite the absorption of ^{18}F-FDG into the systemic circulation and its presence in the kidneys and urinary bladder, no apparent ^{18}F-FDG utilization in the limbs and cardiac muscles was detected. This observation is likely due to the hypoinsulinemia in diabetic rats, resulting in the down-regulation of the number of glucose transporters (Glut4) in these muscle cells (Fig. 6), ultimately diminishing the transport capacity of ^{18}F-FDG [44].

Conversely, the ^{68}Ga-insulin delivered by the EGTA-conjugated NPs was observed not only in the GI tract, but also in the heart, mediastinum, great vessels, kidneys and urinary bladder, which is indicative of systemic absorption of ^{68}Ga-insulin. The radioactivity of ^{18}F-FDG was found in the GI tract, kidneys and urinary bladder; additional radioactivity uptakes were found in the myocardium, and skeletal muscles of chest wall, forelimbs and hindlimbs, suggesting insulin-enhanced glucose utilization in these tissues.

This work also attempted to enable real-time visual monitoring and assessment of their biological processes by superimposing the sequential 3D volume-rendering PET/CT images of ^{68}Ga-insulin (red color) and ^{18}F-FDG (green color) onto the soft-tissue contrast-volume-rendering CT images (gray color, Fig. 7 and Supplementary Video). As shown, the radioactivities of ^{68}Ga-insulin and ^{18}F-FDG (with an approximately 2-h time lag) propagated from the esophagus, stomach through small intestine and, then, accumulated into the systemic circulation after oral ingestion. In response to the stimulation of the absorbed ^{68}Ga-insulin, the ^{18}F-FDG radioactivity uptake was found in the myocardium and skeletal muscles with time. Above results suggest that the ^{68}Ga-insulin delivered by the EGTA-conjugated NPs can be effectively absorbed into the systemic circulation, thus enhancing the ^{18}F-FDG utilization in the insulin-responsive tissues. As is well known, insulin stimulates glucose transport into muscle cells, where it can be stored for future energy use, by enriching the concentration of the glucose transporters (Glut4) at the surface of the cells (Fig. 6) [45].

3.7. PK/PD profiles during OGTT

During OGTT, the SC injection of free-form insulin solution resulted in a maximum plasma concentration at 1 h post administration (the PK profile, Fig. 8a), leading to a sharp decrease in blood glucose levels (the PD profile, Fig. 8b). Conversely, oral administration of DI water or a capsule containing free-form insulin powder produced negligible insulin absorption (Fig. 8a) and insignificant glucose-lowering effects ($P > 0.05$, Fig. 8b). However, orally administering the capsule containing the insulin-loaded EGTA-conjugated NPs revealed a maximum insulin

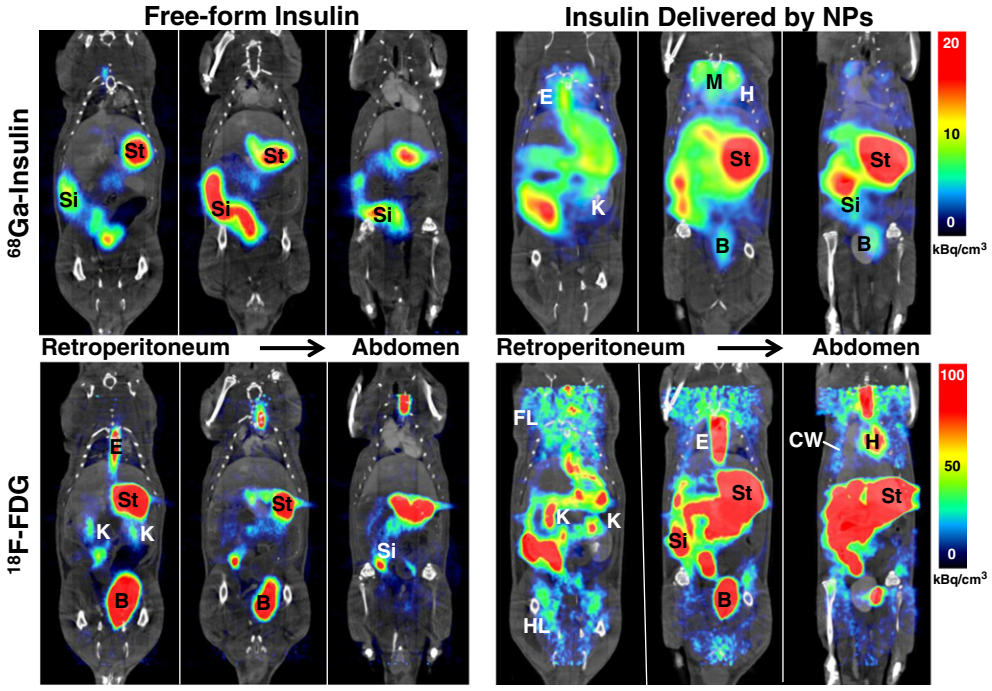

Fig. 5. Biodistribution of ^{68}Ga-insulin (in its free form or delivered by test NPs) and ^{18}F-FDG *via* oral ingestion, illustrated by contrast-enhanced tomographic images. The concentrations of ^{68}Ga-insulin and ^{18}F-FDG in different organs are shown in rainbow pseudo-color scale (kBq/cm^3).

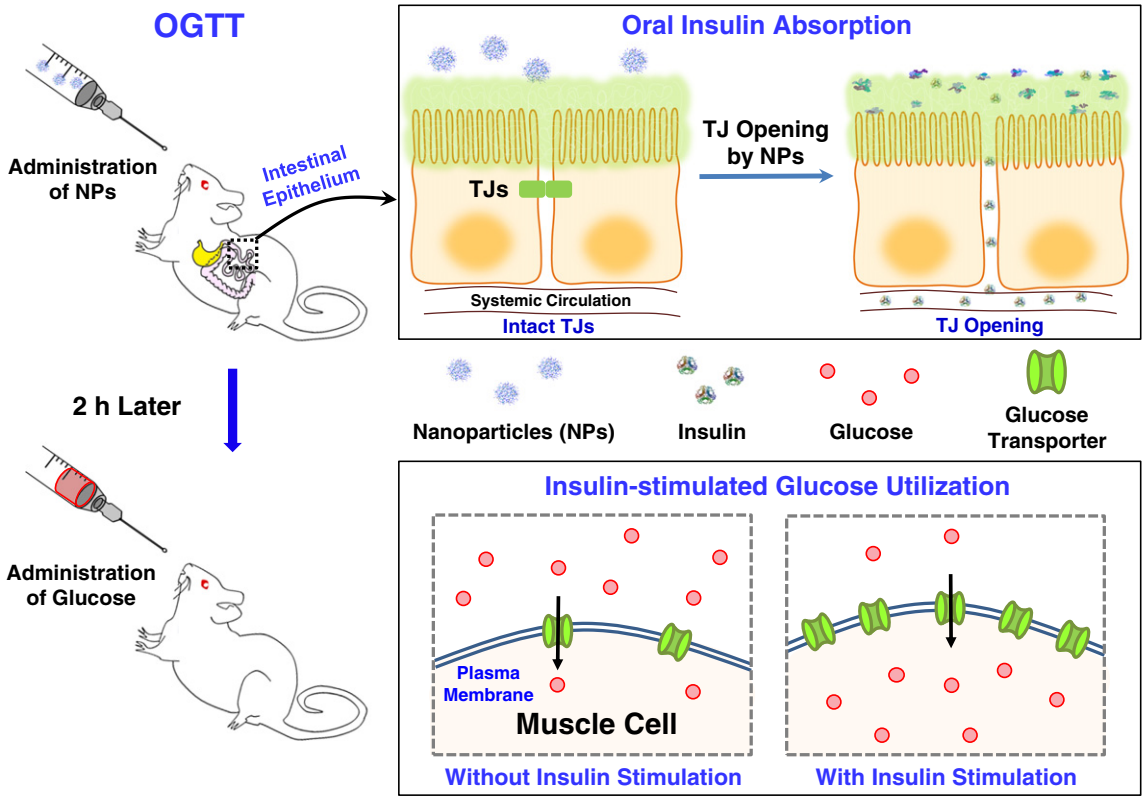

Fig. 6. Schematic diagrams illustrating the procedure of oral glucose tolerance test (OGTT) and the mechanism of test NPs in enhancing the oral absorption of insulin and its subsequent stimulation of glucose utilization in muscle cells. The NPs facilitate paracellular permeability of insulin by disrupting the epithelial TJs; the absorbed insulin enriches the number of glucose transporters at the plasma membrane of muscle cells, resulting in their increased utilization of glucose.

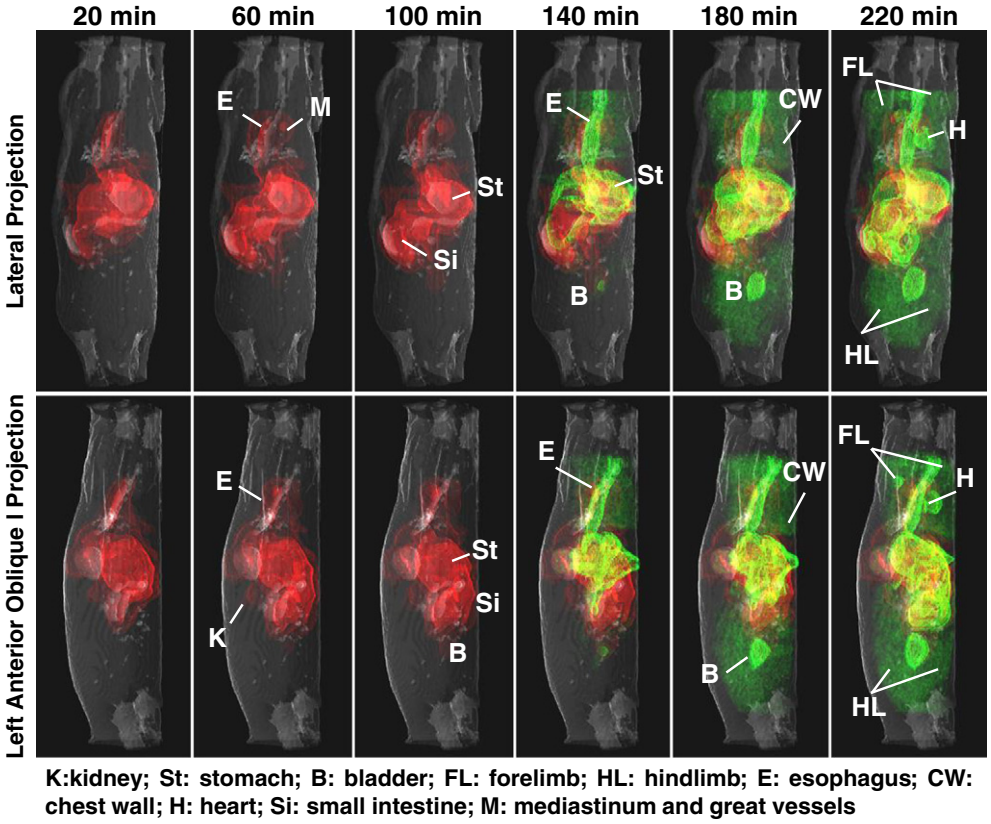

Fig. 7. Soft-tissue contrast CT images (gray color) superimposed with 3D volume-rendering PET fusion images, showing the distribution of ^{68}Ga-insulin (red color, orally delivered by test NPs at time 0) and ^{18}F-FDG (green color, ingested at 2 h post insulin intake) in various body compartments obtained at different time points.

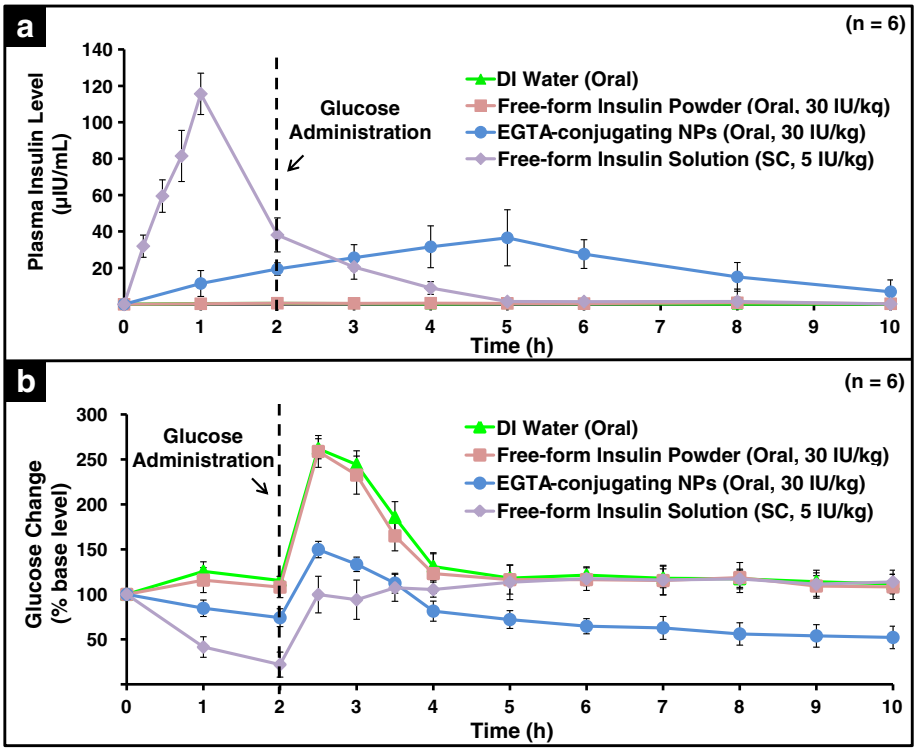

Fig. 8. (a) Plasma insulin level vs. time profiles and (b) blood glucose change vs. time profiles of diabetic rats treated with different formulations of insulin or deionized (DI) water. To mimic the postprandial state, an oral dose of glucose (1 g/kg) was administered to the animals at 2 h after they had received the insulin treatment or DI water. Oral: oral administration; SC: subcutaneous injection.

concentration at 5 h after treatment (the blue line in Fig. 8a), resulting in a significant glucose-lowering effect ($P < 0.05$, Fig. 8b) due to the insulin-mediated glucose utilization (Figs. 5 and 7); its $AUC_{(0–10\ h)}$ was 202.9 ± 32.5 μIU h/mL, and the corresponding BA_R was 17.8 ± 1.3% (Table 1).

4. Conclusions

In this work, a NP carrier system containing EGTA was prepared for oral insulin delivery in diabetic rats during OGTT to mimic the period after a meal. Experimental results indicate that the EGTA-conjugated NPs could enhance the oral absorption of insulin, thus ameliorate postprandial hyperglycemia by facilitating the glucose utilization in the insulin-responsive tissues. Adequately controlling postprandial hyperglycemia helps to reduce the risk of diabetic complications.

Supplementary data to this article can be found online at http://dx.doi.org/10.1016/j.jconrel.2013.05.006.

Table 1
Pharmacokinetic parameters of insulin in diabetic rats following subcutaneous (SC) injection of free-form insulin solution, oral administration of deionized (DI) water, oral administration of a capsule containing free-form insulin powders or insulin-loaded nanoparticles (NPs). C_{max}: maximum plasma concentration; T_{max}: time at which C_{max} is attained; $AUC_{(0–10\ h)}$: area under the plasma concentration–time curve; BA_R: relative bioavailability (n = 6).

	SC free-form insulin solution	Oral DI water	Oral free-form insulin powders	Oral insulin-loaded NPs
Dose (IU/kg)	5.0	0.0	30.0	30.0
C_{max} (μIU/mL)	119.6 ± 3.8	N/A	1.1 ± 0.5	36.5 ± 15.4
T_{max} (h)	1.0	N/A	5.0	5.0
$AUC_{(0–10\ h)}$ (μIU h/mL)	190.0 ± 27.1	N/A	5.8 ± 2.7	202.9 ± 32.5
BA_R (%)	100	N/A	0.1 ± 0.3	17.8 ± 1.3

Acknowledgments

This work was supported by a grant from the National Science Council (NSC 101-2120-M-007-015-CC1), Taiwan, Republic of China. The molecular-imaging study was partially supported by grants from Chang Gung Memorial Hospital (CMRP391513 and CMRPG3A0512).

References

[1] A. Ceriello, Postprandial hyperglycemia and diabetes complications: is it time to treat? Diabetes 54 (2005) 1–7.
[2] P. Mukhopadhyay, R. Mishra, D. Rana, P.P. Kundu, Strategies for effective oral insulin delivery with modified chitosan nanoparticles: a review, Prog. Polym. Sci. 37 (2012) 1457–1475.
[3] H.W. Sung, K. Sonaje, Z.X. Liao, L.W. Hsu, E.Y. Chuang, pH-responsive nanoparticles shelled with chitosan for oral delivery of insulin: from mechanism to therapeutic applications, Acc. Chem. Res. 45 (2012) 619–629.
[4] M.C. Chen, K. Sonaje, K.J. Chen, H.W. Sung, A review of the prospects for polymeric nanoparticle platforms in oral insulin delivery, Biomaterials 32 (2011) 9826–9838.
[5] K. Sonaje, K.J. Lin, J.J. Wang, F.L. Mi, C.T. Chen, J.H. Juang, H.W. Sung, Self-assembled pH-sensitive nanoparticles: a platform for oral delivery of protein drugs, Adv. Funct. Mater. 20 (2010) 3695–3700.
[6] E.Y. Chuang, K.J. Lin, F.Y. Su, H.L. Chen, B. Maiti, Y.C. Ho, T.C. Yen, N. Panda, H.W. Sung, Calcium depletion-mediated protease inhibition and apical-junctional-complex disassembly *via* an EGTA-conjugated carrier for oral insulin delivery, J. Control. Release (2012), http://dx.doi.org/10.1016/j.jconrel.2012.11.011.
[7] M. de Veciana, C.A. Major, M.A. Morgan, T. Asrat, J.S. Toohey, J.M. Lien, A.T. Evans, Postprandial versus preprandial blood glucose monitoring in women with gestational diabetes mellitus requiring insulin therapy, N. Engl. J. Med. 333 (1995) 1237–1241.
[8] P.J. Lefebvre, A.J. Scheen, The postprandial state and risk of cardiovascular disease, Diabet. Med. 15 (Suppl. 4) (1998) S63–S68.
[9] K. Sonaje, Y.J. Chen, H.L. Chen, S.P. Wey, J.H. Juang, H.N. Nguyen, C.W. Hsu, K.J. Lin, H.W. Sung, Enteric-coated capsules filled with freeze-dried chitosan/poly(gamma-glutamic acid) nanoparticles for oral insulin delivery, Biomaterials 31 (2010) 3384–3394.
[10] J. Neefjes, N.P. Dantuma, Fluorescent probes for proteolysis: tools for drug discovery, Nat. Rev. Drug Discov. 3 (2004) 58–69.
[11] T. Huang, K. Huang, A novel insulin derivative chemically modified with dehydrocholic acid: synthesis, characterization and biological activity, Biotechnol. Appl. Biochem. 42 (2005) 47–56.
[12] L. Yin, J. Ding, J. Zhang, C. He, C. Tang, C. Yin, Polymer integrity related absorption mechanism of superporous hydrogel containing interpenetrating polymer networks for oral delivery of insulin, Biomaterials 31 (2010) 3347–3356.

[13] T. Yamagata, M. Morishita, N.J. Kavimandan, K. Nakamura, Y. Fukuoka, K. Takayama, N.A. Peppas, Characterization of insulin protection properties of complexation hydrogels in gastric and intestinal enzyme fluids, J. Control. Release 112 (2006) 343–349.
[14] F.Y. Su, K.J. Lin, K. Sonaje, S.P. Wey, T.C. Yen, Y.C. Ho, N. Panda, E.Y. Chuang, B. Maiti, H.W. Sung, Protease inhibition and absorption enhancement by functional nanoparticles for effective oral insulin delivery, Biomaterials 33 (2012) 2801–2811.
[15] K. Sonaje, E.Y. Chuang, K.J. Lin, T.C. Yen, F.Y. Su, M.T. Tseng, H.W. Sung, Opening of epithelial tight junctions and enhancement of paracellular permeation by chitosan: microscopic, ultrastructural, and computed-tomographic observations, Mol. Pharm. 9 (2012) 1271–1279.
[16] K. Sonaje, K.J. Lin, M.T. Tseng, S.P. Wey, F.Y. Su, E.Y. Chuang, C.W. Hsu, C.T. Chen, H.W. Sung, Effects of chitosan-nanoparticle-mediated tight junction opening on the oral absorption of endotoxins, Biomaterials 32 (2011) 8712–8721.
[17] M. Rekha, C.P. Sharma, Synthesis and evaluation of lauryl succinyl chitosan particles towards oral insulin delivery and absorption, J. Control. Release 135 (2009) 144–151.
[18] J.S. Choi, H.J. Yang, B.S. Kim, J.D. Kim, J.Y. Kim, B. Yoo, K. Park, H.Y. Lee, Y.W. Cho, Human extracellular matrix (ECM) powders for injectable cell delivery and adipose tissue engineering, J. Control. Release 139 (2009) 2–7.
[19] S. Sajeesh, K. Bouchemal, V. Marsaud, C. Vauthier, C.P. Sharma, Cyclodextrin complexed insulin encapsulated hydrogel microparticles: an oral delivery system for insulin, J. Control. Release 147 (2010) 377–384.
[20] W.A. Breeman, A.M. Verbruggen, The ^{68}Ge/^{68}Ga generator has high potential, but when can we use 68Ga-labelled tracers in clinical routine? Eur. J. Nucl. Med. Mol. Imaging 34 (2007) 978–981.
[21] R. Muniyappa, S. Lee, H. Chen, M.J. Quon, Current approaches for assessing insulin sensitivity and resistance *in vivo*: advantages, limitations, and appropriate usage, Am. J. Physiol. Endocrinol. Metab. 294 (2008) E15–E26.
[22] S.L. Aronoff, K. Berkowitz, B. Shreiner, L. Want, Glucose metabolism and regulation: beyond insulin and glucagon, Diabetes Spectr. 17 (2004) 183–190.
[23] K. Sonaje, K.J. Lin, S.P. Wey, C.K. Lin, T.H. Yeh, H.N. Nguyen, C.W. Hsua, T.C. Yen, J.H. Juang, H.W. Sung, Biodistribution, pharmacodynamics and pharmacokinetics of insulin analogues in a rat model: oral delivery using pH-responsive nanoparticles vs. subcutaneous injection, Biomaterials 31 (2010) 6849–6858.
[24] B. Isherwood, P. Timpson, E.J. McGhee, K.I. Anderson, M. Canel, A. Serrels, V.G. Brunton, N.O. Carragher, Live cell *in vitro* and *in vivo* imaging applications: accelerating drug discovery, Pharmaceutics 3 (2011) 141–170.
[25] I. Ihse, P. Lilja, I. Lundquist, Trypsin as a regulator of pancreatic secretion in the rat, Scand. J. Gastroenterol. 14 (1979) 873–880.
[26] Y.H. Lin, K. Sonaje, K.M. Lin, J.H. Juang, F.L. Mi, H.W. Yang, H.W. Sung, Multi-ion-crosslinked nanoparticles with pH-responsive characteristics for oral delivery of protein drugs, J. Control. Release 132 (2008) 141–149.
[27] M. Naraghi, T-jump study of calcium binding kinetics of calcium chelators, Cell Calcium 22 (1997) 255–268.
[28] M. Thanou, J. Verhoef, H. Junginger, Oral drug absorption enhancement by chitosan and its derivatives, Adv. Drug Deliv. Rev. 52 (2001) 117–126.
[29] E. Marttin, J. Verhoef, F. Spies, J. Van der Meulen, J. Nagelkerke, H. Koerten, F. Merkus, The effect of methylated β-cyclodextrins on the tight junctions of the rat nasal respiratory epithelium: electron microscopic and confocal laser scanning microscopic visualization studies, J. Control. Release 57 (1999) 205–213.
[30] A. Zensi, D. Begley, C. Pontikis, C. Legros, L. Mihoreanu, S. Wagner, C. Büchel, H. von Briesen, J. Kreuter, Albumin nanoparticles targeted with Apo E enter the CNS by transcytosis and are delivered to neurones, J. Control. Release 137 (2009) 78–86.
[31] R. Pelletier, The blood–testis barrier: the junctional permeability, the proteins and the lipids, Prog. Histochem. Cytochem. 46 (2011) 49–127.
[32] J. Hochman, P. Artursson, Mechanisms of absorption enhancement and tight junction regulation, J. Control. Release 29 (1994) 253–267.
[33] P.H. Johnson, D. Frank, H.R. Costantino, Discovery of tight junction modulators: significance for drug development and delivery, Drug Discov. Today 13 (2008) 261–267.
[34] M.C. Chen, F.L. Mi, Z.X. Liao, C.W. Hsiao, K. Sonaje, M.F. Chung, L.W. Hsu, H.W. Sung, Recent advances in chitosan-based nanoparticles for oral delivery of macromolecules, Adv. Drug Deliv. Rev. (2012), http://dx.doi.org/10.1016/j.addr.2012.10.010.
[35] A. Allen, G. Flemstrom, A. Garner, E. Kivilaakso, Gastroduodenal mucosal protection, Physiol. Rev. 73 (1993) 823–857.
[36] T. Shimada, Factors affecting the microclimate pH in rat jejunum, J. Physiol. 392 (1987) 113–127.
[37] J.M. Anderson, C.M. Van Itallie, M.D. Peterson, B.R. Stevenson, E.A. Carew, M.S. Mooseker, ZO-1 mRNA and protein expression during tight junction assembly in Caco-2 cells, J. Cell Biol. 109 (1989) 1047–1056.
[38] A. des Rieux, V. Fievez, M. Garinot, Y.J. Schneider, V. Préat, Nanoparticles as potential oral delivery systems of proteins and vaccines: a mechanistic approach, J. Control. Release 116 (2006) 1–27.
[39] M.F. Yam, A. Sadikun, M. Ahmad, G.A. Akowuah, M.Z. Asmawi, Toxicology evaluation of standardized methanol extract of *Gynura procumbens*, J. Ethnopharmacol. 123 (2009) 244–249.
[40] A.M. Alkilany, C.J. Murphy, Toxicity and cellular uptake of gold nanoparticles: what we have learned so far? J. Nanopart. Res. 12 (2010) 2313–2333.
[41] N. Kamei, M. Morishita, Y. Kanayama, K. Hasegawa, M. Nishimura, E. Hayashinaka, Y. Wada, Y. Watanabe, K. Takayama, Molecular imaging analysis of intestinal insulin absorption boosted by cell-penetrating peptides by using positron emission tomography, J. Control. Release 146 (2010) 16–22.
[42] S. Yamashita, T. Takashima, M. Kataoka, H. Oh, S. Sakuma, M. Takahashi, N. Suzuki, E. Hayashinaka, Y. Wada, Y.L. Cui, Y. Watanabe, PET imaging of the gastrointestinal absorption of orally administered drugs in conscious and anesthetized rats, J. Nucl. Med. 52 (2011) 249–256.
[43] V. Kapoor, B.M. McCook, F.S. Torok, An introduction to PET–CT imaging, Radiographics 24 (2004) 523–543.
[44] H. Westergaard, Insulin modulates rat intestinal glucose-transport-effect of hypoinsulinemia and hyperinsulinemia, Am. J. Physiol. 256 (1989) G9113–G9918.
[45] N.J. Bryant, R. Govers, D.E. James, Regulated transport of the glucose transporter GLUT4, Nat. Rev. Mol. Cell Biol. 3 (2002) 267–277.